SUPPLEMENT TO "A MACROECONOMIC MODEL WITH FINANCIALLY CONSTRAINED PRODUCERS AND INTERMEDIARIES"

(*Econometrica*, Vol. 89, No. 3, May 2021, 1361–1418)

VADIM ELENEV
Carey Business School, Johns Hopkins University

TIM LANDVOIGT
The Wharton School, University of Pennsylvania

STIJN VAN NIEUWERBURGH
Graduate School of Business, Columbia University

APPENDIX C: COMPUTATIONAL METHOD

THE EQUILIBRIUM of dynamic stochastic general equilibrium models is usually characterized recursively. If a stationary Markov equilibrium exists, there is a minimal set of state variables that summarizes the economy at any given point in time. Equilibrium can then be characterized using two types of functions: transition functions map today's state into probability distributions of tomorrow's state, and policy functions determine agents' decisions and prices given the current state. Brumm, Kryczka, and Kubler (2018) analyzed theoretical existence properties in this class of models and discussed the literature. Perturbation-based solution methods find local approximations to these functions around the "deterministic steady state." For applications in finance, there are often two problems with local solution methods. First, portfolio restrictions such as leverage constraints may be occasionally binding in the true stochastic equilibrium. Generally, a local approximation around the steady state (with a binding or slack constraint) will therefore inaccurately capture nonlinear dynamics when constraints go from slack to binding. Guerrieri and Iacoviello (2015) proposed a solution using local methods. Second, the portfolio allocation of agents across assets with different risk profiles is generally indeterminate at the nonstochastic steady state. This means that it is generally impossible to solve for equilibrium dynamics using local methods since the point around which to perturb the system is not known.

Global projection methods (Judd (1998)) avoid these problems by not relying on the deterministic steady state. Rather, they directly approximate the transition and policy functions in the relevant area of the state space. An additional advantage of global nonlinear methods is greater flexibility in dealing with highly nonlinear functions within the model such as probability distributions or option-like payoffs.

C.1. *Solution Procedure*

The projection-based solution approach used in this paper has three main steps:

Step 1. *Define approximating basis for the policy and transition functions.* To approximate these unknown functions, we discretize the state space and use multivariate linear interpolation. Our general solution framework provides an object-oriented

Vadim Elenev: velenev@jhu.edu
Tim Landvoigt: timland@wharton.upenn.edu
Stijn Van Nieuwerburgh: svnieuwe@gsb.columbia.edu

 https://doi.org/10.3982/ECTA16438

MATLAB library that allows approximation of arbitrary multivariate functions using linear interpolation, splines, or polynomials. For the model in this paper, splines or polynomials of various orders achieved inferior results due to their lack of global shape preservation.

Step 2. *Iteratively solve for the unknown functions.* Given an initial guess for policy and transition functions, at each point in the discretized state space compute the current-period optimal policies. Using the solutions, compute the next iterate of the transition functions. Repeat until convergence. The system of nonlinear equations at each point in the state space is solved using a standard nonlinear equation solver. Kuhn–Tucker conditions can be rewritten as equality constraints for this purpose. This step is completely parallelized across points in the state space within each iterate.

Step 3. *Simulate the model for many periods using approximated functions.* Verify that the simulated time path stays within the bounds of the state space for which policy and transition functions were computed. Calculate relative Euler equation errors to assess the computational accuracy of the solution. If the simulated time path leaves the state space boundaries or errors are too large, the solution procedure may have to be repeated with optimized grid bounds or positioning of grid points.

We now provide a more detailed description for each step.

C.1.1. *Step 1*

The state space consists of
- two exogenous state variables $[Z_t, \sigma_{\omega,t}]$, and
- five endogenous state variables $[K_t, L_t^P, N_t^I, W_t^S, B_t^G]$.

The state variable L_t^P is aggregate leverage of producers and defined as

$$L_t^P = \frac{q_t^m A_t^P}{p_t K_t}. \tag{C.1}$$

As usual, there are many different possible state variables that encode the same history of aggregate states. We choose this specific set of variables because policy functions turn out to be well-behaved when based on these variables.

We first discretize Z_t into a N^{Z_A}-state Markov chain using the Rouwenhorst (1995) method. The procedure chooses the productivity grid points $\{Z_j\}_{j=1}^{N^{Z_A}}$ and the $N^{Z_A} \times N^{Z_A}$ Markov transition matrix Π_Z between them to match the volatility and persistence of HP-detrended GDP. The dispersion of idiosyncratic productivity shocks $\sigma_{\omega,t}$ can take on two realizations $\{\sigma_{\omega,L}, \sigma_{\omega,H}\}$ as described in the calibration section. The 2×2 Markov transition matrix between these states is given by Π_{σ_ω}. We assume independence between both exogenous shocks. Denote the set of the $N^x = 2N^{Z_A}$ values the exogenous state variables can take on as $\mathcal{S}_x = \{Z_j\}_{j=1}^{N^{Z_A}} \times \{\sigma_{\omega,L}, \sigma_{\omega,H}\}$, and the associated Markov transition matrix $\Pi_x = \Pi_Z \otimes \Pi_{\sigma_\omega}$.

One endogenous state variable can be eliminated for computational purposes since its value is implied by the agents' budget constraints and market clearing conditions, conditional on any four other state variables. We eliminate saver wealth W_t^S, which can be computed as

$$W_t^S = \Omega_A\big(\omega_t^*\big)\big(1 + \delta q_t^m\big)A_t^P + M_t - N_t^I + B_t^G.$$

Our solution algorithm requires approximation of continuous functions of the endogenous state variables. Define the "true" endogenous state space of the model as follows: if each endogenous state variable $S_t \in \{K_t, A_t^P, N_t^I, B_t^G\}$ can take on values in a continuous and convex subset of the reals, characterized by constant state boundaries, $[\bar{S}_l, \bar{S}_u]$, then the endogenous state space $\mathcal{S}_n = [\bar{K}_l, \bar{K}_u] \times [\bar{L}_l^P, \bar{L}_u^P] \times [\bar{N}_l^I, \bar{N}_u^I] \times [\bar{B}_l^G, \bar{B}_u^G]$. The total state space is the set $\mathcal{S} = \mathcal{S}_x \times \mathcal{S}_n$.

To approximate any function $f : \mathcal{S} \to \mathcal{R}$, we form a univariate grid of (not necessarily equidistant) strictly increasing points for each endogenous state variable, that is, we choose $\{K_j\}_{j=1}^{N_K}$, $\{L_k^P\}_{k=1}^{N_L}$, $\{N_m^I\}_{m=1}^{N_I}$, and $\{B_n^G\}_{n=1}^{N_G}$. These grid points are chosen to ensure that each grid covers the ergodic distribution of the economy in its dimension, and to minimize computational errors, with more details on the choice provided below. Denote the set of all endogenous-state grid points as $\hat{\mathcal{S}}_n = \{K_j\}_{j=1}^{N_K} \times \{L_k^P\}_{k=1}^{N_P} \times \{N_m^I\}_{m=1}^{N_I} \times \{B_n^G\}_{n=1}^{N_G}$, and the total discretized state space as $\hat{\mathcal{S}} = \mathcal{S}_x \times \hat{\mathcal{S}}_n$. This discretized state space has $N^S = N^x \cdot N^K \cdot N^P \cdot N^I \cdot N^G$ total points, where each point is a 5×1 vector as there are five distinct state variables. We can now approximate the smooth function f if we know its values $\{f_j\}_{j=1}^{N^S}$ at each point $\hat{s} \in \hat{\mathcal{S}}$, that is, $f_j = f(\hat{s}_j)$ by multivariate linear interpolation.

Our solution method requires approximation of three sets of functions defined on the domain of the state variables. The first set of unknown functions $\mathcal{C}_P : \mathcal{S} \to \mathcal{P} \subseteq \mathcal{R}^{N^C}$, with N^C being the number of policy variables, determines the values of endogenous objects specified in the equilibrium definition at every point in the state space. These are the prices, agents' choice variables, and the Lagrange multipliers on the portfolio constraints. Specifically, the 15 policy functions are bond prices $q^m(\mathcal{S})$, $q^f(\mathcal{S})$, investment $X(\mathcal{S})$, consumption $c^B(\mathcal{S})$, $c^S(\mathcal{S})$, non-financial firm equity issuance $e^P(\mathcal{S})$, bank equity issuance $e^I(\mathcal{S})$, wages $w^B(\mathcal{S})$, $w^S(\mathcal{S})$, the choice of loans and corporate bonds of banks and savers $A^I(\mathcal{S})$ and $A^S(\mathcal{S})$, the Lagrange multipliers for the bank leverage constraint $\lambda^I(\mathcal{S})$ and no-shorting constraint $\mu^I(\mathcal{S})$, the multiplier for firms' leverage constraint $\lambda^P(\mathcal{S})$, and finally the multiplier on the savers' no-shorting constraint $\mu^S(\mathcal{S})$. There is an equal number of these unknown functions and nonlinear functional equations, to be listed under step 2 below.

The second set of functions $\mathcal{C}_T : \mathcal{S} \times \mathcal{S}_x \to \mathcal{S}_n$ determine the next-period endogenous state variable realizations as a function of the state in the current period and the next-period realization of exogenous shocks. There is one transition function for each endogenous state variable, corresponding to the transition law for each state variable, also to be listed below in step 2.

The third set are forecasting functions $\mathcal{C}_F : \mathcal{S} \to \mathcal{F} \subseteq \mathcal{R}^{N^F}$, where N^F is the number of forecasting variables. They map the state into the set of variables sufficient to compute expectations terms in the nonlinear functional equations that characterize equilibrium. They partially coincide with the policy functions, but include additional functions. In particular, the forecasting functions for our model are the bond price $q^m(\mathcal{S})$, investment $X(\mathcal{S})$, consumption $c^B(\mathcal{S})$, $c^S(\mathcal{S})$, bank equity issuance $e^I(\mathcal{S})$, the value functions of households $V^S(\mathcal{S})$, $V^B(\mathcal{S})$, and banks $V^I(\mathcal{S})$, and the wage bill $w(\mathcal{S}) = w^B(\mathcal{S}) + w^S(\mathcal{S})$.

C.1.2. *Step 2*

Given an initial guess $\mathcal{C}^0 = \{\mathcal{C}_P^0, \mathcal{C}_T^0, \mathcal{C}_F^0\}$, the algorithm to compute the equilibrium takes the following steps.

A. *Initialize* the algorithm by setting the current iterate $\mathcal{C}^m = \{\mathcal{C}_P^m, \mathcal{C}_T^m, \mathcal{C}_F^m\} = \{\mathcal{C}_P^0, \mathcal{C}_T^0, \mathcal{C}_F^0\}$.

B. *Compute forecasting values.* For each point in the discretized state space, $s_j \in \hat{\mathcal{S}}$, $j = 1, \ldots, N^S$, perform the steps:
   i. Evaluate the transition functions at s_j combined with each possible realization of the exogenous shocks $x_i \in \mathcal{S}_x$ to get $s'_j(x_i) = \mathcal{C}_T^m(s_j, x_i)$ for $i = 1, \ldots, N^x$, which are the values of the endogenous state variables given the current state s_j and for each possible future realization of the exogenous state.
   ii. Evaluate the forecasting functions at these future state variable realizations to get $f_{i,j}^0 = \mathcal{C}_F^m(s'_j(x_i), x_i)$.

   The end result is a $N^x \times N^S$ matrix $\mathcal{F}^m$, with each entry being a vector

$$f_{i,j}^m = \left[q_{i,j}^m, C_{i,j}^B, C_{i,j}^S, e_{i,j}^I, V_{i,j}^B, V_{i,j}^S, V_{i,j}^I, X_{i,j}, w_{i,j}\right] \tag{F}$$

   of the next-period realization of the forecasting functions for current state s_j and future exogenous state x_i.

C. *Solve system of nonlinear equations.* At each point in the discretized state space, $s_j \in \hat{\mathcal{S}}$, $j = 1, \ldots, N^S$, solve the system of nonlinear equations that characterize equilibrium in the equally many "policy" variables, given the forecasting matrix $\mathcal{F}^m$ from step B. This amounts to solving a system of 15 equations in 15 unknowns:

$$\hat{P}_j = \left[\hat{q}_j^m, \hat{q}_j^f, \hat{X}_j, \hat{c}_j^B, \hat{c}_j^S, \hat{e}_j^P, \hat{e}_j^I, \hat{A}_j^I, \hat{A}_j^S, \hat{w}_j^B, \hat{w}_j^S, \hat{\lambda}_j^I, \hat{\mu}_j^I, \hat{\lambda}_j^P, \hat{\mu}_j^S\right] \tag{P}$$

   at each s_j. The equations are

$$\begin{aligned}\hat{q}_j^m = \hat{\lambda}_j^P F + \mathrm{E}_{s'_{i,j}|s_j}\Bigg\{\hat{\mathcal{M}}_{i,j}^P\Bigg[&\left(1 - F_{\omega,i}\left(\omega_{i,j}^*\right)\right)\left(1 - (1-\theta)\tau^{\Pi} + \delta q_{i,j}^m\right) \\ &+ \frac{f_{\omega,i}\left(\omega_{i,j}^*\right)\Pi\left(\omega_{i,j}^*\right)}{Z_i \hat{\tilde{k}}_j^{1-\alpha} \hat{\tilde{l}}_j^{\alpha}}\Bigg]\Bigg\},\end{aligned} \tag{E1}$$

$$\begin{aligned}\hat{p}_j\left(1 - \Phi\hat{\lambda}_j^P\right) = \mathrm{E}_{s'_{i,j}|s_j}\Bigg[\hat{\mathcal{M}}_{i,j}^P\Bigg\{&p_{i,j}\left(1 - F_{\omega,i}\left(\omega_{i,j}^*\right)\right)\left(\left(1-\tau^{\Pi}\right)\mathrm{M\hat{P}K}_{i,j}\omega_{i,j}^+ \right. \\ &\left. + (1-\delta_K)\,p_{i,j} - \left(1-\tau^{\Pi}\right)\varsigma\right) \\ &- \frac{f_{\omega,i}\left(\omega_{i,j}^*\right)\Pi\left(\omega_{i,j}^*\right)}{Z_i \hat{\tilde{k}}_j^{1-\alpha} \hat{\tilde{l}}_j^{\alpha}}\left(\varsigma - \mathrm{M\hat{P}K}_{i,j}\omega_{i,j}^*\right)\Bigg\}\Bigg],\end{aligned} \tag{E2}$$

$$\begin{aligned}&(1-\tau_{\Pi})\left(1 - F_{\omega,i}\left(\hat{\omega}_j^*\right)\right)\left(\hat{\omega}_j^+ \mathrm{M\hat{P}L}_j^B - \hat{w}_j^B\right) \\ &\quad = f_{\omega,j}\left(\hat{\omega}_j^*\right)\Pi\left(\hat{\omega}_j^*, \hat{\tilde{k}}_j, \hat{\tilde{a}}_j^P, \mathcal{S}_t\right)\frac{\partial\hat{\omega}_j^*}{\partial\hat{\tilde{l}}_j^B},\end{aligned} \tag{E3}$$

$$\begin{aligned}&(1-\tau_{\Pi})\left(1 - F_{\omega,i}\left(\hat{\omega}_j^*\right)\right)\left(\hat{\omega}_j^+ \mathrm{M\hat{P}L}_j^S - \hat{w}_j^S\right) \\ &\quad = f_{\omega,j}\left(\hat{\omega}_j^*\right)\Pi\left(\hat{\omega}_j^*, \hat{\tilde{k}}_j, \hat{\tilde{a}}_j^P, \mathcal{S}_t\right)\frac{\partial\hat{\omega}_j^*}{\partial\hat{\tilde{l}}_j^S},\end{aligned} \tag{E4}$$

$$\hat{q}_j^f + \tau^{\Pi}\hat{r}_j^f - \kappa = \hat{q}_j^f\hat{\lambda}_j^I + \mathrm{E}_{s'_{i,j}|s_j}\left[\hat{\mathcal{M}}_{i,j}^I\right], \tag{E5}$$

$$\hat{q}_j^m = \xi \hat{\lambda}_j^I \hat{q}_j^m + \hat{\mu}_j^I + \mathrm{E}_{s'_{i,j}|s_j}\big[\hat{\mathcal{M}}_{i,j}^I\big(M_{i,j} + \delta q_{i,j}^m\big(1 - F_{\omega,i}\big(\omega_{i,j}^*\big)\big)\big)\big], \tag{E6}$$

$$\hat{q}_j^f = \hat{\mu}_j^S + \mathrm{E}_{s'_{i,j}|s_j}\big[\hat{\mathcal{M}}_{i,j}^S\big], \tag{E7}$$

$$\begin{aligned}\hat{q}_j^m + \big(\Psi^S\big)'\big(\hat{A}_j^S\big) \\ = \hat{\mu}_j^S + \mathrm{E}_{s'_{i,j}|s_j}\big[\hat{\mathcal{M}}_{i,j}^S\big(M_{i,j} + \big(1 - F_{\omega,i}\big(\omega_{i,j}^*\big)\big)\big(1 + \delta q_{i,j}^m\big)\big)\big],\end{aligned} \tag{E8}$$

$$\big(\Phi \hat{p}_j \hat{\bar{k}}_j - F \hat{\tilde{a}}_j^P\big)\hat{\lambda}_j^P = 0, \tag{E9}$$

$$\big(\xi \hat{q}_j^m \hat{A}_j^I - \hat{q}_j^f \hat{B}_j^I\big)\hat{\lambda}_j^I = 0, \tag{E10}$$

$$\hat{A}_j^I \hat{\mu}_j^I = 0, \tag{E11}$$

$$\hat{A}_j^S \hat{\mu}_j^S = 0, \tag{E12}$$

$$\hat{B}_j^S = B_j^G + \hat{B}_j^I, \tag{E13}$$

$$\hat{A}_j^P = \hat{A}_j^S + \hat{A}_j^I, \tag{E14}$$

$$\begin{aligned}\hat{c}_j^B = \hat{D}_j^P + \hat{D}_j^I + \big(1 - \tau_t^B\big)\hat{w}_j^B \bar{L}^B + \hat{G}_j^{T,B} \\ + \hat{p}_j \hat{X}_j - \hat{X}_j - \Psi(\hat{X}_j, K_j).\end{aligned} \tag{E15}$$

Equations (E1) and (E2) are the Euler equations for borrower-entrepreneurs from (A.14) and (A.15). Equations (E3) and (E4) are the intratemporal optimality conditions for labor demand by borrower-entrepreneurs from (A.13). Equations (E5) and (E6) are the Euler equations for banks from (A.31) and (A.30). Equations (E7) and (E8) are the savers' Euler equations for short-term and corporate bonds, (A.39) and (A.40). Equations (E9) and (E10) are the leverage constraints (2.8) and (A.23) for borrowers and banks, respectively. Equations (E11) and (E12) are the no-shorting constraints (A.24) and (A.34) for banks and savers, respectively. Equations (E13) and (E14) are the market clearing condition for riskfree debt and corporate bonds respectively, (2.22) and (2.23). Finally, E(15) is the borrower's budget constraint, (2.3).

Expectations are computed as weighted sums, with the weights being the probabilities of transitioning to exogenous state x_i, conditional on state s_j. Hats ($\hat{\cdot}$) in (E1)–E(15) indicate variables that are direct functions of the vector of unknowns (P). These are effectively the choice variables for the nonlinear equation solver that finds the solution to the system (E1)–(E15) at each point s_j. All variables in the expectation terms with subscript $_{i,j}$ are direct functions of the forecasting variables (F).

These values are *fixed* numbers when the system is solved, as they were precomputed in step B. For example, the stochastic discount factors $\hat{\mathcal{M}}_{i,j}^h$, $h = B, I, S$, depend on both the solution and the forecasting vector, for example, for savers,

$$\hat{\mathcal{M}}_{i,j}^S = \beta_S \left(\frac{V_{i,j}^S}{CE_j^S}\right)^{1/\nu_S - \sigma_S} \left(\frac{c_{i,j}^S}{\hat{c}_j^S}\right)^{-1/\nu_S},$$

since they depend on future consumption and indirect utility, but also current consumption. To compute the expectation of the right-hand side of equation (E7) at

point s_j, we first look up the corresponding column j in the matrix containing the forecasting values that we computed in step B, $\mathcal{F}^m$. This column contains the N^x vectors, one for each possible realization of the exogenous state, of the forecasting values defined in (F). From these vectors, we need saver consumption $c^S_{i,j}$ and the saver value function $V^S_{i,j}$. Further, we need current consumption $\hat{c}^S_j$, which is a policy variable chosen by the nonlinear equation solver. Denoting the probability of moving from current exogenous state x_j to state x_i as $\pi_{i,j}$, we compute the certainty equivalent

$$CE^S_j = \left[\sum_{x_i|x_j} \pi_{i,j} \left(V^S_{i,j}\right)^{1-\sigma_S}\right]^{\frac{1}{1-\sigma_S}},$$

and then complete expectation of the RHS of (E7)

$$\mathrm{E}_{s'_{i,j}|s_j}\left[\hat{\mathcal{M}}^S_{i,j}\right] = \sum_{x_i|x_j} \pi_{i,j} \beta_S \left(\frac{V^S_{i,j}}{CE^S_j}\right)^{1/\nu_S - \sigma_S} \left(\frac{c^S_{i,j}}{\hat{c}^S_j}\right)^{-1/\nu_S}.$$

The mapping of solution and forecasting vectors (P) and (F) into the other expressions in equations (E1)–E(15) follows the same principles and is based on the definitions in Model Appendix A. For example, the borrower default threshold is a function of current wages and state variables based on (2.5):

$$\hat{\omega}^*_j = \frac{\hat{w}^B_j l^B + \hat{w}^S_j l^S + a^P_j + \varsigma k_j}{Z_i (k_j)^{1-\alpha} l^\alpha},$$

and the capital price is a linear function of investment from the first-order condition (A.3):

$$\hat{p}_j = 1 + \psi\left(\frac{\hat{X}_j}{k_j} - \delta_K\right).$$

The system (E1)–(E15) implicitly uses the budget constraints of non-financial and financial firms, savers, and the government to compute several variables as direct function of the state and policy variables.

Note that we could exploit the linearity of the budget constraint in (E15) to eliminate one more policy variable, $\hat{c}^B_j$, from the system analytically. However, in our experience the algorithm is more robust when we explicitly include consumption of all agents as policy variables, and ensure that these variables stay strictly positive (as required with power utility) when solving the system. To solve the system in practice, we use a nonlinear equation solver that relies on a variant of Newton's method, using policy functions $\mathcal{C}^m_P$ as initial guess. More on these issues in Section C.2 below.

The final output of this step is an $N^S \times 15$ matrix $\mathcal{P}^{m+1}$, where each row is the solution vector $\hat{P}_j$ that solves the system (E1)–E(15) at point s_j.

D. *Update forecasting, transition, and policy functions.* Given the policy matrix $\mathcal{P}^{m+1}$ from step B, update the policy function directly to get $\mathcal{C}^{m+1}_P$. All forecasting functions with the exception of the value functions are also equivalent to policy functions. Value functions are updated based on the recursive definitions

$$\hat{V}^S_j = \left\{(1-\beta_S)\left[\hat{c}^S_j\right]^{1-1/\nu} + \beta_S \mathrm{E}_{s'_{i,j}|s_j}\left[\left(V^S_{i,j}\right)^{1-\sigma_S}\right]^{\frac{1-1/\nu}{1-\sigma_S}}\right\}^{\frac{1}{1-1/\nu}}, \tag{V1}$$

$$\hat{V}_j^B = \left\{(1-\beta_B)\left[\hat{c}_j^B\right]^{1-1/\nu} + \beta_B \mathrm{E}_{s'_{i,j}|s_j}\left[\left(V_{i,j}^B\right)^{1-\sigma_B}\right]^{\frac{1-1/\nu}{1-\sigma_B}}\right\}^{\frac{1}{1-1/\nu}}, \tag{V2}$$

$$\hat{V}_j^I = \phi_0^I N_j^I - \hat{e}_j^I + \mathrm{E}_{s'_{i,j}|s_j}\left[\hat{\mathcal{M}}_{i,j}^B (1-F_{\epsilon,i,j})\left(V_{i,j}^I + \epsilon_{i,j}^{I,+}\right)\right], \tag{V3}$$

using the same notation as defined above under step C. Note that each value function combines current solutions from $\mathcal{P}^{m+1}$ (step C) for consumption and equity issuance with forecasting values from $\mathcal{F}^m$ (step B). Using these updated value functions, we get $\hat{\mathcal{C}}_F^{m+1}$.

Finally, update transition functions for the endogenous state variables using the following laws of motion, for current state s_j and future exogenous state x_i as defined above:

$$K_{i,j} = (1-\delta_K)K_j + \hat{X}_j, \tag{T1}$$

$$L_{i,j}^P = \frac{q_{i,j}\hat{A}_j^P}{p_{i,j}K_j}, \tag{T2}$$

$$N_{i,j}^I = \left(M_{i,j} + \delta q_{i,j}^m\left(1-F_{\omega,i}\left(\omega_{i,j}^*\right)\right)\right)\hat{A}_j^I - \hat{B}_j^I, \tag{T3}$$

$$B_{i,j}^G = \frac{1}{\hat{q}_j^f}\left(B_j^G + \hat{G}_j - \hat{T}_j\right). \tag{T4}$$

Equation (T1) is simply the law of motion for aggregate capital, and (T2) follows from the definition of producer leverage in (C.1). Equation (T3) is the law of motion for bank net worth (A.22). Equations (T2) and (T3) combine inputs from old forecasting functions $\mathcal{F}^m$ and new policy solutions $\mathcal{P}^{m+1}$. Equation (T4) is the government budget constraint (2.21). Updating according to (T1)–(T4) gives the next set of functions $\hat{\mathcal{C}}_T^{m+1}$.

E. *Check convergence.* Compute distance measures $\Delta_F = \|\mathcal{C}_F^{m+1} - \mathcal{C}_F^m\|$ and $\Delta_T = \|\mathcal{C}_T^{m+1} - \mathcal{C}_T F^m\|$. If $\Delta_F < \mathrm{Tol}_F$ and $\Delta_T < \mathrm{Tol}_T$, stop and use $\mathcal{C}^{m+1}$ as approximate solution. Otherwise reset policy functions to the next iterate, that is, $\mathcal{P}^m \to \mathcal{P}^{m+1}$, and reset forecasting and transition functions to a convex combination of their previous and updated values, that is, $\mathcal{C}^m \to \mathcal{C}^{m+1} = D \times \mathcal{C}^m + (1-D) \times \hat{\mathcal{C}}^{m+1}$, where D is a dampening parameter set to a value between 0 and 1 to reduce oscillation in function values in successive iterations. Next, go to step B.

C.1.3. *Step 3*

Using the numerical solution $\mathcal{C}^* = \mathcal{C}^{m+1}$ from step 2, we simulate the economy for $\bar{T} = T_{ini} + T$ period. Since the exogenous shocks follow a discrete-time Markov chain with transition matrix Π_x, we can simulate the chain given any initial state x_0 using $\bar{T}-1$ uniform random numbers based on standard techniques (we fix the seed of the random number generator to preserve comparability across experiments). Using the simulated path $\{x_t\}_{t=1}^{\bar{T}}$, we can simulate the associated path of the endogenous state variables given initial state $s_0 = [x_0, K_0, L_0^P, N_0^I, W_0^S, B_0^G]$ by evaluating the transition functions

$$\left[K_{t+1}, L_{t+1}^P, N_{t+1}^I, W_{t+1}^S, B_{t+1}^G\right] = \mathcal{C}_T^*(s_t, x_{t+1}),$$

to obtain a complete simulated path of model state variables $\{s_t\}_{t=1}^{\bar{T}}$. To remove any effect of the initial conditions, we discard the first T_{ini} points. We then also evaluate the policy

and forecasting functions along the simulated sample path to obtain a complete sample path $\{s_t, P_t, f_t\}_{t=1}^{\bar{T}}$.

To assess the quality and accuracy of the solution, we perform two types of checks. First, we verify that all state variable realizations along the simulated path are within the bounds of the state variable grids defined in step 1. If the simulation exceeds the grid boundaries, we expand the grid bounds in the violated dimensions, and restart the procedure at step 1. Second, we compute relative errors for all equations of the system (E1)–E(15) and the transition functions (T1)–(T4) along the simulated path. For equations involving expectations (such as (E1)), this requires evaluating the transition and forecasting function as in step 2B at the current state s_t. For each equation, we divide both sides by a sensibly chosen endogenous quantity to yield "relative" errors; for example, for (E1) we compute

$$1-\frac{1}{\hat{q}_j^m}\left(\hat{\lambda}_j^P F+\mathrm{E}_{s'_{i,j}|s_j}\left\{\hat{\mathcal{M}}_{i,j}^P\left[\left(1-F_{\omega,i}\left(\omega_{i,j}^*\right)\right)\left(1-(1-\theta)\tau^{\Pi}+\delta q_{i,j}^m\right)+\frac{f_{\omega,i}\left(\omega_{i,j}^*\right)\Pi\left(\omega_{i,j}^*\right)}{Z_i\hat{\tilde{k}}_j^{1-\alpha}\hat{\tilde{l}}_j^{\alpha}}\right]\right\}\right),$$

using the same notation as in step 2B. These errors are small by construction when calculated at the points of the discretized state grid $\hat{\mathcal{S}}$, since the algorithm under step 2 solved the system exactly at those points. However, the simulated path will likely visit many points that are between grid points, at which the functions $\mathcal{C}^*$ are approximated by interpolation. Therefore, the relative errors indicate the quality of the approximation in the relevant area of the state space. We report average, median, and tail errors for all equations. If errors are too large during simulation, we investigate in which part of the state space these high errors occur. We then add additional points to the state variable grids in those areas and repeat the procedure.

C.2. *Implementation*

Solving the System of Equations. We solve a system of nonlinear equations at each point in the state space using a standard nonlinear equation solver (MATLAB's fsolve). This nonlinear equation solver uses a variant of Newton's method to find a "zero" of the system. We employ several simple modifications of the system (E1)–E(15) to avoid common pitfalls at this step of the solution procedure. Nonlinear equation solvers are notoriously bad at dealing with complementary slackness conditions associated with constraint, such as (E9)–E(12). Judd, Kubler, and Schmedders (2002) discussed the reasons for this and also showed how Kuhn–Tucker conditions can be rewritten as additive equations for this purpose. For example, consider the bank's Euler equation for risk-free bonds and the Kuhn–Tucker condition for its leverage constraint:

$$\hat{q}_j^f\left(1-\hat{\lambda}_j^I\right)+\tau^{\Pi}\hat{r}_j^f-\kappa=\mathrm{E}_{s'_{i,j}|s_j}\left[\hat{\mathcal{M}}_{i,j}^I\right],$$
$$\left(\xi\hat{q}_j^m\hat{A}_j^I-\hat{q}_j^f\hat{B}_j^I\right)\hat{\lambda}_j^I=0.$$

Now define an auxiliary variable $h_j\in\mathcal{R}$ and two functions of this variable, such that $\hat{\lambda}_j^{I,+}=\max\{0,h_j\}^3$ and $\hat{\lambda}_j^{I,-}=\max\{0,-h_j\}^3$. Clearly, if $h_j<0$, then $\hat{\lambda}_j^{I,+}=0$ and $\hat{\lambda}_j^{I,-}>0$, and vice versa for $h_j>0$. Using these definitions, the two equations above can be transformed to

$$\hat{q}_j^f\left(1-\hat{\lambda}_j^{I,+}\right)+\tau^{\Pi}\hat{r}_j^f-\kappa=\mathrm{E}_{s'_{i,j}|s_j}\left[\hat{\mathcal{M}}_{i,j}^I\right], \tag{K1}$$

$$\xi\hat{q}_j^m\hat{A}_j^I-\hat{q}_j^f\hat{B}_j^I-\hat{\lambda}_j^{I,-}=0. \tag{K2}$$

The solution variable for the nonlinear equation solver corresponding to the multiplier is h_j. The solver can choose positive h_j to make the constraint binding ($\hat{\lambda}_j^{I,-} = 0$), in which case $\hat{\lambda}_j^{I,+}$ takes on the value of the Lagrange multiplier. Or the solver can choose negative h_j to make the constraint non-binding ($\hat{\lambda}_j^{I,+} = 0$), in which case $\hat{\lambda}_j^{I,-}$ can take on any value that makes (K2) hold.

Similarly, certain solution variables are restricted to positive values due to the economic structure of the problem. For example, with power, utility consumption must be positive. To avoid that, the solver tries out negative consumption values (and thus utility becomes ill-defined); we use $\log(\hat{c}_j^n)$, $n = B, S$, as solution variable for the solver. This means the solver can make consumption arbitrarily small, but not negative.

The nonlinear equation solver needs to compute the Jacobian of the system at each step. Numerical central-difference (forward-difference) approximation of the Jacobian can be inaccurate and is computationally costly because it requires $2N + 1$ ($N + 1$) evaluations of the system, with N being the number of variables, whereas analytically computed Jacobians are exact and require only one evaluation. We follow Elenev (2016) in "pre-computing" all forecasting functions in step 2B of the algorithm, so that we can calculate the Jacobian of the system analytically. To do so, we employ the Symbolic Math Toolbox in MATLAB, passing the analytic Jacobian to fsolve at the beginning of step 2C. This greatly speeds up calculations.

Grid Configuration. Recall that one endogenous state variable can be eliminated because of the adding-up property of budget constraints in combination with market clearing. We choose to eliminate saver wealth W^S. The grid points in each state dimension are as follows:

- *Z:* We discretize Z_t into a 5-state Markov chain using the Rouwenhorst (1995) method. The procedure chooses the productivity grid points $\{Z_j\}_{j=1}^5$ and the 5×5 Markov transition matrix Π_Z between them to match the volatility and persistence of HP-detrended GDP. This yields the possible realizations: [0.957, 0.978, 1.000, 1.022, 1.045].
- σ_ω: [0.1, 0.18] (see calibration)
- *K:* [1.60, 1.75, 1.84, 1.98, 2.05, 2.10, 2.26, 2.40]
- L^P: [0.23, 0.30, 0.33, 0.35, 0.37, 0.39, 0.40, 0.41, 0.42, 0.43, 0.44, 0.46, 0.47, 0.48, 0.49, 0.5, 0.55]
- N^I:

$$[-0.040, -0.030, -0.020, -0.010, 0.000, 0.005, 0.010, 0.015, 0.020, 0.025, 0.030, \ldots$$
$$\ldots 0.035, 0.040, 0.045, 0.050, 0.055, 0.060, 0.065, 0.070, 0.080, 0.090, 0.100, \ldots$$
$$\ldots 0.120, 0.140, 0.160, 0.200, 0.270]$$

- B^G: [0.183, 0.467, 0.750, 1.033, 1.317, 1.400, 1.700].

The total state space grid has 257,040 points. As pointed out by several previous studies such as Kubler and Schmedders (2003), portfolio constraints lead to additional computational challenges since portfolio policies may not be smooth functions of state variables due to occasionally binding constraints. Hence we cluster grid points in areas of the state space where constraints transition from slack to binding. Our policy functions are particularly nonlinear in bank net worth N^I, since the status of the bank leverage constraint (binding or not binding) depends predominantly on this state variable. To achieve acceptable accuracy, we have to specify a very dense grid for N^I, as can be seen above. Also note

that the lower end of the N^I grid includes some negative values. Negative realizations of N^I can occur in severe financial crisis episodes. Recall that N^I is the beginning-of-period net worth of all banks. Depending on the realization of their idiosyncratic payout shock, banks decide whether or not to default. Thus, the model contains two reasons why banks may not default despite initial negative net worth: (i) positive idiosyncratic shocks, and (ii) positive franchise value. The lower bound of N^I needs to be low enough such that bank net worth is not artificially truncated during crises, but it must not be so low that, given such low initial net worth, banks cannot be recapitalized to get back to positive net worth. Thus, the "right" lower bound depends on the strength of the equity issuance cost and other parameters. Finding the right value for the lower bound is a matter of experimentation.

Generating an Initial Guess and Iteration Scheme. To find a good initial guess for the policy, forecasting, and transition functions, we solve the deterministic "steady state" of the model under the assumption that the bank leverage constraint is binding and government debt/GDP is 60%. We then initialize all functions to their steady-state values, for all points in the state space. Note that the only role of the steady-state calculation is to generate an initial guess that enables the nonlinear equation solver to find solutions at (almost) all points during the first iteration of the solution algorithm. In our experience, the steady state delivers a good enough initial guess.

In case the solver cannot find solutions for some points during the initial iterations, we revisit such points at the end of each iteration. We try to solve the system at these "failed" points using as initial guess the solution of the closest neighboring point at which the solver was successful. This method works well to speed up convergence and eventually find solutions at all points.

To further speed up computation time, we run the initial 100 iterations with a coarser state space grid (19,500 points total). After these iterations, the algorithm is usually close to convergence; however, the accuracy during simulation would be too low. Therefore, we initialize the finer (final) solution grid using the policy, forecasting, and transition function obtained after 100 coarse grid iterations. We then run the algorithm for at most 30 more iterations on the fine grid.

To determine convergence, we check absolute errors in the value functions of households and banks, (V1)–V(3). Out of all functions we approximate during the solution procedure, these exhibit the slowest convergence. We stop the solution algorithm when the maximum absolute difference between two iterations, and for all three functions and all points in the state space, falls below 1e-3 and the mean distance falls below 1e-4. For appropriately chosen grid boundaries, the algorithm will converge within the final 30 iterations.

In some cases, our grid boundaries are wider than necessary, in the sense that the simulated economy never visits the areas near the boundary on its equilibrium path. Local convergence in those areas is usually very slow, but not relevant for the equilibrium path of the economy. If the algorithm has not achieved convergence after the 30 additional iterations on the fine grid, we nonetheless stop the procedure and simulate the economy. If the resulting simulation produces low relative errors (see step 3 of the solution procedure), we accept the solution. After the 130 iterations described above, our simulated model economies either achieve acceptable accuracy in relative errors, or if not, the cause is a badly configured state grid. In the latter case, we need to improve the grid and restart the solution procedure. Additional iterations, beyond 100 on the coarse and 30 on the fine grid, do not change any statistics of the simulated equilibrium path for any of the simulations we report.

We implement the algorithm in MATLAB and run the code on a high-performance computing (HPC) cluster. As mentioned above, the nonlinear system of equations can be solved in parallel at each point. We parallelize across 28 CPU cores of a single HPC node. From computing the initial guess and analytic Jacobian to simulating the solved model, the total running time for the benchmark calibration is about 1 hour and 30 minutes.

Simulation. To obtain the quantitative results, we simulate the model for 10,000 periods after a "burn-in" phase of 500 periods. The starting point of the simulation is the ergodic mean of the state variables. As described in detail above, we verify that the simulated time path stays within the bounds of the state space for which the policy functions were computed. We fix the seed of the random number generator so that we use the same sequence of exogenous shock realizations for each parameter combination.

To produce impulse response function (IRF) graphs, we simulate 10,000 different paths of 25 periods each. In the initial period, we set the endogenous state variables to several different values that reflect the ergodic distribution of the states. We use a clustering algorithm to represent the ergodic distribution nonparametrically. We fix the initial exogenous shock realization to mean productivity ($Z = 1$) and low uncertainty ($\sigma_{\omega,\text{low}}$). The "impulse" in the second period is either only a bad productivity shock ($Z = 0.978$) for non-financial recessions, or both low Z and a high uncertainty shock ($\sigma_{\omega,hi}$) for financial recessions. For the remaining 23 periods, the simulation evolves according to the stochastic law of motion of the shocks. In the IRF graphs, we plot the median path across the 10,000 paths given the initial condition.

C.3. *Evaluating the Solution*

Equation Errors. Our main measure to assess the accuracy of the solution are relative equation errors calculated as described in step 3 of the solution procedure. Table S.I reports the median error, the 95th percentile of the error distribution, the 99th, and the 100th percentiles during the 10,000 period simulation of the model. Median and 75th percentile errors are small for all equations. Maximum errors are on the order of 2% for equations (E5)–(E6). These errors are caused by a suboptimal approximation of the bank's Lagrange multiplier λ^I in rarely occurring states. It is possible to reduce these errors by placing more grid points in those areas of the state space. In our experience, adding points to eliminate the tail errors has little to no effect on any of the results we report. Since it increases computation times nonetheless, we chose the current grid configuration.

Policy Function Plots. We further visually inspect policy functions to gauge whether the approximated functions have the smoothness and monotonicity properties implied by our choices of utility and adjustment cost functions. Such plots also allow us to see the effect of binding constraints on prices and quantities. For example, Figure S.1 shows investment by firms and the Lagrange multiplier on the bank's leverage constraint. It is obvious from the graphs that a binding intermediary constraint restricts investment. The intermediary constraint becomes binding for low values of intermediary net worth. Further note the interaction with borrower-entrepreneur net worth: holding fixed intermediary net worth, the constraint is more likely to become biding for low borrower wealth.

State Space Histogram Plots. We also create histogram plots for the endogenous state variables, overlaid with the placement of grid points. These types of plots allow us to check

TABLE S.I

COMPUTATIONAL ERRORS[a]

Equation		*Percentile*				
		50th	75th	95th	99th	Max
E1	(A.14)	0.0010	0.0012	0.0022	0.0068	0.0179
E2	(A.15)	0.0003	0.0004	0.0007	0.0024	0.0062
E3	(A.13), B	0.0001	0.0003	0.0003	0.0003	0.0003
E4	(A.13), S	0.0001	0.0003	0.0003	0.0003	0.0003
E5	(A.31)	0.0020	0.0040	0.0098	0.0125	0.0187
E6	(A.30)	0.0015	0.0036	0.0098	0.0128	0.0190
E7	(A.39)	0.0001	0.0002	0.0005	0.0008	0.0012
E8	(A.40)	0.0002	0.0005	0.0014	0.0020	0.0029
E9	(2.8)	0.0039	0.0047	0.0052	0.0056	0.0091
E10	(A.23)	0.0003	0.0003	0.0004	0.0005	0.0020
E11	(A.24)	0.0000	0.0000	0.0000	0.0000	0.0003
E12	(A.34)	0.0004	0.0005	0.0007	0.0008	0.0010
E13	(2.22)	0.0000	0.0000	0.0000	0.0001	0.0002
E14	(2.23)	0.0000	0.0000	0.0000	0.0000	0.0000
E15	(2.3)	0.0015	0.0025	0.0050	0.0105	0.0251
T1		0.0000	0.0000	0.0000	0.0000	0.0000
T2	(C.1)	0.0003	0.0004	0.0006	0.0010	0.0040
T3	(A.22)	0.0004	0.0005	0.0008	0.0014	0.0103
T4	(2.21)	0.0002	0.0003	0.0003	0.0005	0.0031

[a]The table reports median, 75th percentile, 95th percentile, 99th percentile, and maximum absolute value errors, evaluated at state space points from a 10,000 period simulation of the benchmark model. Each row contains errors for the respective equation of the nonlinear system (E1)–(E15) listed in step 2 of the solution procedure, and the transition equations for the state variables (T1)–(T4). The table's second column contains corresponding equation numbers in the main text and Appendix A.

that the simulated path of the economy does not violate the state grid boundaries. It further helps us to determine where to place grid points. Histogram plots for the benchmark economy are in Figure S.2.

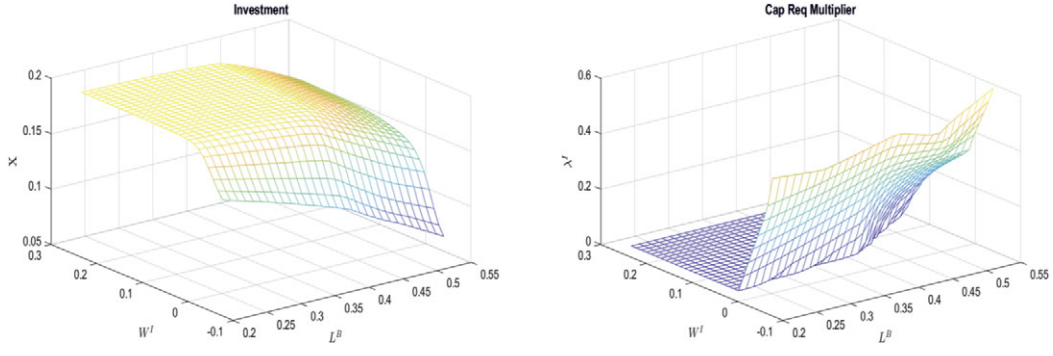

FIGURE S.1.—Plot of optimal investment and Lagrange multiplier on bank leverage constraint. The left panel plots investment by borrower-entrepreneurs as function of borrower-entrepreneur wealth W^B and bank net worth N^I. The right panel plots the Lagrange multiplier on the bank leverage constraint for the same state variables. Both plots are for the benchmark economy. The other state variables are fixed to the following values: $Z = 1$, $\sigma_\omega = \bar{\sigma}_{\omega,L}$, $K^B = 2.3$, $B^G = 0.5$.

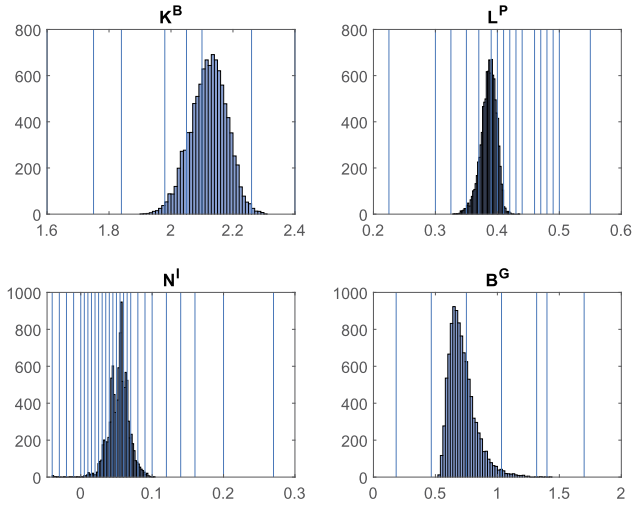

FIGURE S.2.—Histogram plots of endogenous state variables. The plots show histograms for capital and borrower-entrepreneur wealth in the top row, and intermediary net worth and government debt in the bottom row, for the 10,000 period simulation of the benchmark economy. The vertical lines indicate the values of grid points.

APPENDIX D: CALIBRATION APPENDIX

D.1. *Bank Payouts and Leverage*

Dividend Payout and Equity Issuance. We construct the equity issuance and payout series using Compustat and CRSP data. Following Baron (2020), we define banks as firms engaging in "depository credit intermediation" (NAICS codes beginning with 5221). For the period before NAICS were introduced, we consider firms with SIC codes between 6020 and 6036. We discard all bank-quarters in which a bank's assets or equity grew by more than 20% to avoid attributing equity-financed M&A to repurchases or issuances. Baron (2020) used a lower cutoff of 10%. The 20% cutoff is more robust for our calculation, since it is less likely to produce false positives, particularly in the immediate aftermath of the crisis when the largest banks grew rapidly.

Further following Baron (2020), we construct time series of dividends, share repurchases, and equity issuances as percent of book equity aggregating across all publicly traded banks. Because a bank may both issue and repurchase equity in the same year, we examine monthly changes in split- and stock-dividend-adjusted shares outstanding across all of a bank's share classes using CRSP data. Repurchases are negative changes in shares outstanding, multiplied by the end-of-month adjusted price. Issuances are positive changes. This procedure could still produce downwards-biased estimates of both if a company issues and repurchases shares within the same month, but this is less of a concern than at lower frequencies. We construct dividends as Compustat's dividends-per-share multiplied by shares outstanding, aggregate across all banks in a given year, and divide by aggregate bank book equity at the end of the previous year.

To ensure comprehensive coverage, we restrict the sample to 1974 through 2018. Over this period, banks paid out an average of 6.8% of their book equity per year as dividends plus share repurchases, and issued 4.8% as new equity. In the data, banks raise equity in part to finance trend balance sheet expansion, which averages 3.7% in real terms. Since our model is stationary, we target issuance net of asset growth. This yields a net payout

TABLE S.II

BALANCE SHEET VARIABLES AND PRICES

		Dec 2014			Avg 53-14
Table	*Sector*	*Assets*	*Liabilities*	*Leverage*	*Leverage*
L.111	U.S.-Chartered Depository Institutions	$13,647	$12,161	0.891	0.921
L.112	Foreign Banking Offices in U.S.	$2093	$2086	0.996	1.065
L.113	Banks in U.S.-Affiliated Areas	$92	$88	0.953	1.080
L.114	Credit Unions	$1066	$958	0.899	0.916
	Subtotal: Banks	$16,898	$15,292	0.905	0.928
L.125	Government-Sponsored Enterprises (GSEs)	$6400	$6387	0.998	0.971
L.126	Agency- and GSE-Backed Mortgage Pools	$1649	$1649	1.000	1.000
L.127	Issuers of Asset-Backed Securities (ABS)	$1424	$1424	1.000	1.003
L.129.m	Mortgage Real Estate Investment Trusts	$568	$483	0.851	0.955
L.128	Finance Companies	$1501	$1376	0.916	0.873
L.130	Security Brokers and Dealers	$3255	$1345	0.413	0.808
L.131	Holding Companies	$4391	$2103	0.479	0.441
L.132	Funding Corporations	$1305	$1305	1.000	1.000
	Subtotal: Other Liquidity Providers	$20,492	$16,070	0.784	0.872
L.116	Life Insurance Companies	$6520	$5817	0.892	0.932
	Total	$43,910	$37,179	0.847	*0.915*
L.121	Money-Market Mutual Funds	$2725	$2725	1.000	1.000
L.129.e	Equity Real Estate Investment Trusts	$157	$539	3.427	2.577
	Total (K-VJ Definition)	$40,271	$33,549	0.833	0.909

ratio (dividends + repurchases - issuances + real asset growth rate), which is 5.8% on average and pro-cyclical with a volatility of 6.0%. The gross payout ratio of 6.8% directly pins down ϕ_0^I, and we target a net payout ratio if 5.8% by setting $\phi_1^I = 7$.

Measuring Intermediary Sector Leverage. Our notion of the intermediary sector is the levered financial sector. We take book values of assets and liabilities of these sectors from the Financial Accounts of the United States (formerly Flow of Funds). We subtract holding and funding company equity investments in subsidiaries from those subsidiaries' liabilities. Table S.II reports the assets, liabilities, and leverage of each sector as of 2014, as well as the average leverage from 1953 to 2014. We find that the average leverage ratio of the levered financial sector was 91.5%. This is our calibration target.

Krishnamurthy and Vissing-Jorgensen (2015) identified a similar group of financial institutions as net suppliers of safe, liquid assets. Their financial sector includes money market mutual funds (which do not perform maturity transformation) and equity REITS (which operate physical assets) but excludes life insurance companies (which are highly levered). The financial sector definition of Krishnamurthy and Vissing-Jorgensen (2015) suggests a similar ratio of 90.9%. As an aside, we note that Krishnamurthy and Vissing-Jorgensen (2015) reported lower total assets and liabilities than in our reconstruction of their procedure because they net out positions within the financial sector by instrument while we do not.

D.2. *Non-Financial Corporate Payouts and Leverage*

Dividend Payout and Equity Issuance. We compute a time series of aggregate payouts by non-financial firms in a similar way as for banks. Our goal is to calculate aggregate an-

nual payouts—dividends and share repurchases—by public non-financial firms as a fraction of the previous year's aggregate book equity. As is standard in the literature, we use all Compustat firms except regulated utilities (SIC codes 4000–4999) and financial services firms (SIC codes 6000–6999).

Like we do for banks, we use the 1974–2018 sample and discard firm-quarters in which equity grew by more than 20% to exclude equity-financed M&A. Share repurchases are monthly declines in shares outstanding. On average, from 1974 to 2018, the non-financial sector paid out 7.8% of its equity value in dividends and repurchases and issued 3.1% of new equity. Firms issue equity in part to finance growth. Unlike for banks, non-financial firms' assets/GDP remain stable; however, the data still feature real growth. Because our model is stationary, we calculate issuance as net of real GDP growth, which averages 1.7% in our sample. This yields a net payout ratio = repurchases + dividends - issuance + real GDP growth. Its mean is 6.4%, and it is pro-cyclical with a volatility of 3.1%. The gross payout ratio of 7.8% directly pins down ϕ_0, and we target a net payout ratio if 6.4% by setting $\beta_B = 0.94$.

Measuring Non-Financial Leverage. We define the non-financial sector as the aggregate of the non-financial corporate and non-financial non-corporate business sectors in the Financial Accounts of the United States (formerly Flow of Funds). We construct leverage as the ratio of loans plus debt securities to non-financial assets using the following FRED identifiers:

$$\text{Leverage} = \frac{\text{TCMILBSNNCB} + \text{NNBDILNECL} + \text{OLALBSNNB} + \text{NNBTML}}{\text{TTAABSNNCB} + \text{TTAABSNNB}}.$$

Non-financial leverage steadily increases until the mid-1980s. To ensure we are calculating the average of a stationary series, we start our sample in 1985. From then until 2015, leverage is acyclical with a mean of 36.9% and a volatility of 3.4%.

D.3. *Measuring the Household Share*

In our model, non-financial firm debt can be held either by the levered financial sector or by households directly. The empirical counterpart to non-financial firm debt is domestic corporate bonds and loans. The counterpart to household holdings includes both debt held by households as well as debt held by non-levered (e.g., pass-through) intermediaries. To construct this series, we turn to the Financial Accounts of the United States (formerly Flow of Funds).

There are two empirical challenges. First, foreign investors, who do not have a counterpart in our model, own an appreciable share of corporate bonds. Second, reported household holdings of "corporate and foreign bonds" include asset-backed securities, bonds issued by financial firms, and bonds issued by foreign entities. To deal with these challenges, we reconstruct aggregates from Table L.213 as follows, using market values (codes beginning with LM) over book values (codes beginning with FL) where available. An example of this calculation for December 2014 is presented in Table S.III.

We begin with total corporate and foreign bonds in the economy, issued by either non-financial firms, the levered financial sector (including ABS), or rest of the world. When these assets are held by a financial firm, the FoF breaks down the holding into ABS and other, allowing us to exclude these holdings from the calculation. We then use the liability portion of the table to compute the fraction of remaining corporate and foreign

TABLE S.III

MEASURING THE HOUSEHOLD SHARE OF NON-FINANCIAL FIRM DEBT

		Example: December 2014	
FoF Data Code	*Description*	*Value from FoF*	*Scaled*
FL893163005	Total Corporate and Foreign Bonds	12,097,540	
	Less Identifiable Holdings of ABS and MBS		
LM763063605	U.S.-chartered depository institutions	138,820	
LM473063605	Credit Unions	10,952	
LM513063605	Property-Casualty Insurance Companies	98,840	
LM543063675	Life Insurance Companies	465,741	
FL403063605	Government-Sponsored Enterprises	79,819	
LM263063603	Rest of the World	405,130	
	Subtotal	1,199,302	
	Remaining Corporate and Foreign Bonds	10,898,238	
FL103163003	Bonds Issued by the Non-Fin Corp Sector	4,554,756	
	Fraction Issued by Non-Fin Corp Sector		41.8%
	Broadly Defined Household Sector		
LM153063005	Households	1,627,149	680,043
LM573063005	Private Pension Funds	698,600	291,969
LM343063005	Federal Pension Funds	12,086	5051
LM223063045	State & Local Pension Funds	579,039	242,001
LM653063005	Mutual Funds	1,823,312	762,026
LM553063003	Closed-End Funds	75,783	31,672
LM563063003	Exchange-Traded Funds	231,911	96,924
	Subtotal		2,109,686
	Levered Financial Sector		
LM763063095	U.S.-chartered depository institutions	386,950	161,720
LM753063005	Foreign banking offices in U.S.	190,787	79,737
LM743063005	Banks in U.S.-affiliated areas	5367	2243
LM473063095	Credit unions	194	81
LM513063095	Property-casualty insurance companies	358,528	149,841
LM543063095	Life insurance companies	1,966,899	822,036
FL633063005	Money Market Funds	68,588	28,665
FL403063095	Government-sponsored enterprises	5970	2495
LM613063003	Finance companies	68,839	28,770
FL643063005	REITs	38,922	16,267
FL663063005	Brokers and dealers	114,534	47,868
LM733063003	Holding companies	29,179	12,195
FL503063005	Funding corporations	77,891	32,553
	Subtotal		1,384,472
FL144123005	Loans Issued by Nonfinancial Business		6,940,354
	Household Share		20.22%

bonds that were issued by the non-financial sector and *assume* that all investors hold non-financial sector issued corporate bonds in the same proportion as the total.

This allows us to compute holdings of non-financial sector issued corporate bonds by each of the FoF sectors. We classify these sectors into (1) rest of the world, (2) "levered financial sector" consistent with our computation of financial sector leverage in Section D.1, and (3) a broadly defined "household sector," which includes FoF Household Sector, as well as pension funds (private, federal, state, and local) and pass-through investment funds (MMFs, mutual funds, closed-end funds, and ETFs).

Finally, we compute the household share of non-financial firm debt as the amount of non-financial sector corporate bonds held by the broadly defined household sector divided by the sum of total non-financial sector corporate bonds held by (1) households and (2) levered financial sector, as well as (3) loans taken out by nonfinancial corporate and noncorporate business. According to Table L.216, there are small amounts—for example, $24.3 billion in Dec 2014—of loans to non-financial firms held by the household sector. We do not include these in the numerator of our saver share because it is difficult for households to own whole loans, so these are likely held by some financial intermediaries, for example, hedge funds, that the FoF treats as part of the household sector.

D.4. *Parameter Sensitivity Analysis*

In a complex, nonlinear structural general equilibrium model like ours, it is often difficult to see precisely which features of the data drive the ultimate results. This appendix follows the approach advocated by Andrews, Gentzkow, and Shapiro (2017) to report how key moments are affected by changes in the model's key parameters, in the hope of improving the transparency of the results. Structural identification of parameters and sensitivity of results are two sides of the same coin.

Consider a generic vector of moments $\mathbf{m}$ which depends on a generic parameter vector $\boldsymbol{\theta}$. Let $\boldsymbol{\iota}_i$ be a selector vector of the same length as $\boldsymbol{\theta}$ taking a value of 1 in the ith position and zero elsewhere. Denote the parameter choices in the benchmark calibration by a superscript b. For each parameter θ_i, we solve the model once for $\theta^b \circ e^{\iota_i \varepsilon}$ and once for $\theta^b \circ e^{-\iota_i \varepsilon}$. We then report the symmetric finite difference:

$$\frac{\log\left(\mathbf{m}\left(\theta^b \circ e^{\iota_i \varepsilon}\right)\right) - \log\left(\mathbf{m}\left(\theta^b \circ e^{\iota_i \varepsilon}\right)\right)}{2\varepsilon}.$$

We set $\varepsilon = 0.01$, or 1% of the benchmark parameter value. The resulting quantities are elasticities of moments to structural parameters.

We report the sensitivity of the first 16 target moments in Table II to the 16 parameters in the first 16 rows of that table. Those are all parameters calibrated inside the model except for fiscal policy parameters which are identified almost directly by their corresponding fiscal policy target moment. Each panel of Figure S.3 lists the same 16 moments and shows the elasticity of the moments to one of the 16 parameters. For consistency, we report percentage changes, which are unit-free, in every moment. The movements in the bank bankruptcy rate in response to multiple parameters appear to be large, but they are only large relative to a small baseline bank bankruptcy rate of 0.63% per year.

Some parameters are identified mainly by their target moment. When more resources seized from a defaulting producer are lost to the lender (higher ζ^P), loss severities on corporate loans increase. Raising the savers' target holdings of corporate bonds φ_0 increases their share held by savers, while making it costlier for savers to deviate from that target (higher φ_1) reduces the share's volatility.

Others affect the results in more complex ways. Many parameters that make the economy riskier decrease bank net payouts, because banks choose to retain earnings out of precaution. These include higher capital adjustment costs ψ, which make Tobin's q more volatile, and higher persistence ρ_Z and volatility σ_Z of TFP shocks. This effect can be seen best in the ϕ_1^I panel. Making it costlier for banks to raise equity mechanically decreases issuance and hence increases net payouts in crises. However, banks anticipate this and retain more earnings ex ante, which both decreases net payouts and increases their net worth. Both effects serve to lower the ratio.

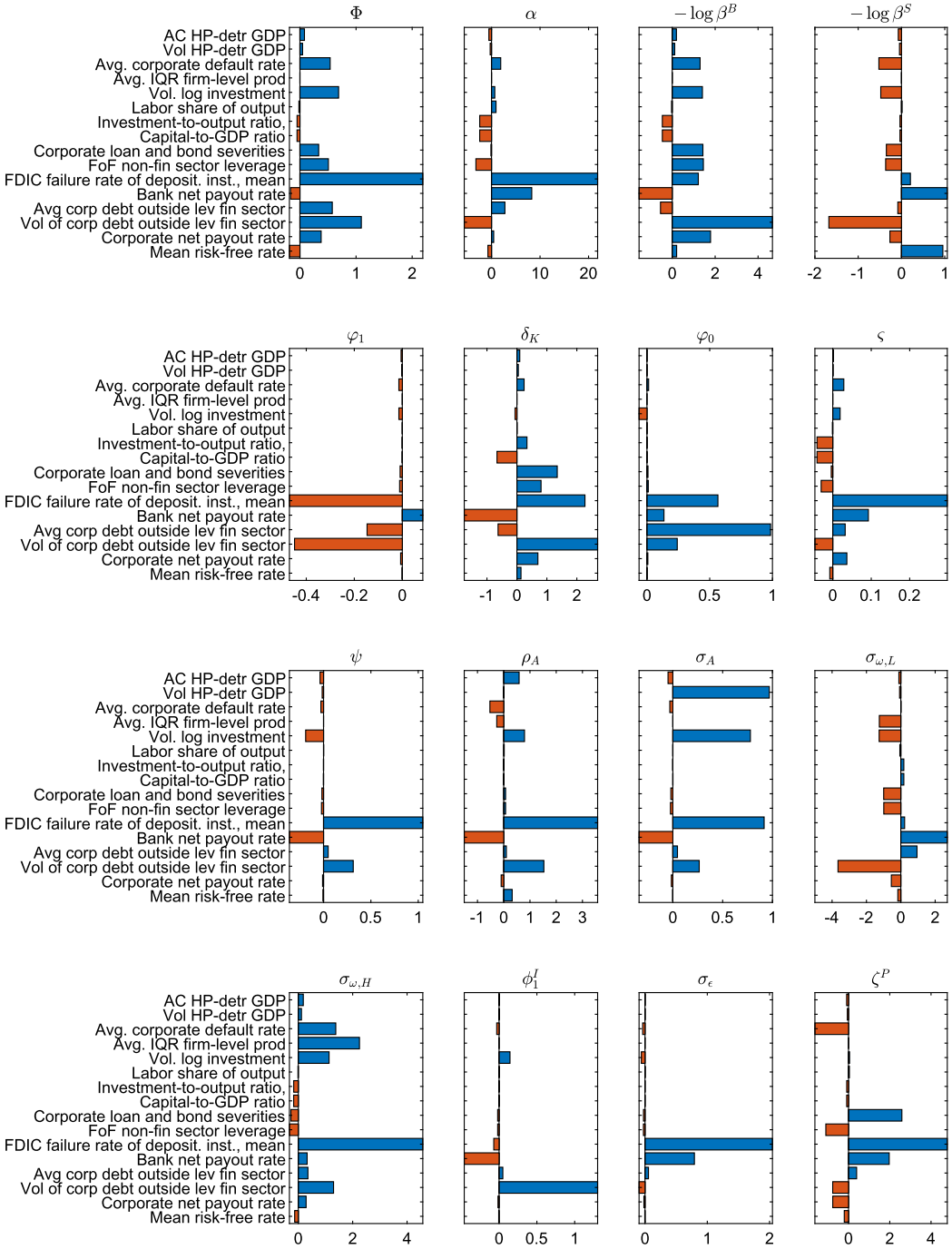

FIGURE S.3.—Parameter sensitivity analysis. *Blue line:* non-financial recession *Red line:* financial recession.

Banks also decrease their payouts when the volatility of idiosyncratic bank shocks σ_ϵ *decreases*, in part because the decrease makes the economy riskier—corporate defaults and volatility of investment are higher. As the financial sector becomes more efficient at sharing risk within itself, it take on more systemic risk in the aggregate, making it more vulnerable in the aggregate.

Last, an important driver of intermediation in our model is the difference in discount rates between borrowers (high) and savers (low). When this difference increases, for example, when the discount rate of borrowers $-\log\beta_B$ goes up, so does firm leverage, making it substantially riskier with more corporate defaults and more volatile investment. Inversely, when the difference decreases, for example, when the discount rate of savers $-\log\beta_S$ moves closer to that of the borrowers, there is less debt and lower risk. In Appendix B.5, we check if our results are robust to changes in β_B and β_S that would decrease the intermediation motive. They are.

D.5. *Long-Term Corporate Bonds*

Our model's corporate bonds are geometrically declining perpetuities, and as such have no principal. The issuer of one unit of the bond at time t promises to pay the holder 1 at time $t+1$, δ at time $t+2$, δ^2 at time $t+3$, and so on. Issuers must hold enough capital to collateralize the face value of the bond, given by $F=\frac{\theta}{1-\delta}$, a constant parameter that does not depend on any state variable of the economy. Real-life bonds have a finite maturity and a principal payment. They also have a vintage (year of issuance), whereas our bonds combine all vintages in one variable. This appendix explains how to map the geometric bonds in our model into real-world bonds by choosing values for δ and θ.

Our model's corporate loan/bond refers to the entire pool of all outstanding corporate loans/bonds. To proxy for this pool, we use investment-grade and high-yield indices constructed by Bank of America Merill Lynch (BofAML) and Barclays Capital (BarCap). For the BofAML indices (Datastream Codes LHYIELD and LHCCORP for investment grade and high-yield corporate bonds, respectively), we obtain a time series of monthly market values, durations (the sensitivity of prices to interest rates), weighted-average maturity (WAM), and weighted average coupons (WAC) for January 1997 until December 2015. For the BarCap indices (C0A0 and H0A0 for investment grade and high-yield corporate bonds, respectively), we obtain a time series of option-adjusted spreads over the Treasury yield curve.

First, we use market values of the BofAML investment grade and high-yield portfolios to create an aggregate bond index and find its mean WAC c of 5.5% and WAM T of 10 years over our time period. We also add the time series of OAS to the constant maturity treasury rate corresponding to that period's WAM to get a time series of bond yields r_t. Next, we construct a plain vanilla corporate bond with a semiannual coupon and maturity equal to the WAC and WAM of the aggregate bond index, and compute the price for \$1 par of this bond for each yield:

$$P^c(r_t)=\sum_{i=1}^{2T}\frac{c/2}{(1+r_t)^{i/2}}+\frac{1}{(1+r_t)^T}.$$

We can write the steady-state price of a geometric bond with parameter δ as

$$P^G(r_t)=\frac{1}{1+r_t}\big[1+\delta P^G(r_t)\big].$$

Solving for $P^G(y_t)$, we get

$$P^G(r_t) = \frac{1}{1 + r_t - \delta}.$$

The calibration determines how many units X of the geometric bond with parameter δ one needs to sell to hedge one unit of plain vanilla bond P^c against parallel shifts in interest rates, across the range of historical yields:

$$\min_{\delta, X} \sum_{t=1997.1}^{2015.12} \left[P^c(r_t) - X P^G(r_t; \delta)\right]^2.$$

We estimate $\delta = 0.937$ and $X = 12.9$, yielding an average pricing error of only 0.41%. This value for δ implies a time series of durations $D_t = -\frac{1}{P_t^G}\frac{dP_t^G}{dr_t}$ with a mean of 6.84.

To establish a notion of principal for the geometric bond, we compare it to a duration-matched zero-coupon bond, that is, borrowing some amount today (the principal) and repaying it D_t years from now. The principal of this loan is just the price of the corresponding D_t maturity zero-coupon bond $\frac{1}{(1+r_t)^{D_t}}$

We set the "principal" F of one unit of the geometric bond to be some fraction θ of the undiscounted sum of all its cash flows $\frac{\theta}{1-\delta}$, where

$$\theta = \frac{1}{N} \sum_{t=1997.1}^{2015.12} \frac{1}{(1 + r_t)^{D_t}}.$$

We get $\theta = 0.582$ and $F = 9.18$.

D.6. *Measuring Labor Income Tax Revenue*

We define income tax revenue as current personal tax receipts (line 3) plus current taxes on production and imports (line 4) minus the net subsidies to government sponsored enterprises (line 30 minus line 19) minus the net government spending to the rest of the world (line 25 + line 26 + line 29 − line 6 − line 9 − line 18). Our logic for adding the last three items to personal tax receipts is as follows. Taxes on production and export mostly consist of federal excise and state and local sales taxes, which are mostly paid by consumers. Net government spending on GSEs consists mostly of housing subsidies received by households which can be treated equivalently as lowering the taxes that households pay. Finally, in the data, some of the domestic GDP is sent abroad in the form of net government expenditures to the rest of the world rather than being consumed domestically. Since the model has no foreigners, we reduce personal taxes for this amount, essentially rebating this lost consumption back to domestic agents.

D.7. *Taxation of Savers' Financial Income*

Savers earn financial income from two sources. First, they earn interest on their private lending, that is, deposits in the financial intermediaries. This income is ultimately a claim on the capital rents in the economy and should be taxed at the same rate τ_K as borrowers' and intermediaries' net income.

Second, they earn interest on their public lending, that is, government bonds. In the data, Treasury coupons are taxed at the household's marginal tax rate, τ in the model.

However, the tax revenue collected by the government from interest income on its own bonds is substantially lower than τB_t^G because (a) Treasury coupons are exempt from state and local taxes, and (b) more than half of privately owned Treasury debt is held by foreigners, who also do not pay federal income taxes.

In the model, there is one tax rate τ_D at which all of the saver's interest income is taxed. We choose τ_D to satisfy

$$\tau_D\big(\hat{B}^I + \hat{B}^G\big) = \tau^K\big(\hat{B}^I - \hat{B}^I_{\text{pension}}\big) + \tau\frac{\hat{\tau}^{\text{federal}}}{\hat{\tau}^{\text{total}}}\big(\hat{B}^G - \hat{B}^G_{\text{foreign}} - \hat{B}^I_{\text{pension}}\big),$$

where hats denote quantities in the data. Specifically, the revenue from taxes collected at rate τ_D on all private safe debt and government debt must equal the sum of tax revenues collected on taxable private safe debt (private safe debt not held in tax-advantaged pension funds) at rate τ_K, and tax revenues collected on taxable public debt (Treasury debt not held by foreigners, the Fed, or pension funds) taxed at rate $\tau\frac{\hat{\tau}^{\text{federal}}}{\hat{\tau}^{\text{total}}}$.

We measure all quantities at December 31, 2014. Private debt stocks are taken from the Financial Accounts of the United States. Treasury debt stocks are taken from the Treasury Bulletin. Federal and total personal tax revenues are taken from the BEA's National Income and Product Accounts. There is approximately \$13 trillion each outstanding of private and public debt. Almost all private debt is taxable, but only \$4 trillion of public debt is. Federal taxes constitute approximately 80% of all personal income tax revenue. Using the calibration for τ_K and τ, we get

$$\tau_D \approx \frac{20\% \times \$13T + 29.5\% \times 0.8 \times \$4T}{\$13T + \$13T}$$

or $\tau_D = 13.4\%$ precisely.

D.8. *Stationarity of Government Debt*

In our numerical work, we guarantee the stationarity of government debt by gradually lowering the tax rate when debt falls (profligacy) and raising it when debt rises (austerity). The labor income tax rate $\tau_t^B = \tau_t^S = \tau_t$ is the target rate τ multiplied by the term $\exp b_\tau z_t$ in order to capture the cyclicality of labor tax revenue. To enforce stationarity, we set the target tax rate τ as follows:

$$\tau = \tau_0\left(\frac{B_t^G - \underline{B}^G}{B_{ss}^G - \underline{B}^G}\right)^{b_G}.$$

We set $\underline{B}^G = -0.4$ to allow debt (as a fraction of steady-state output normalized to 1) to be in the $[-0.4, 0]$ region without getting a complex number for the tax rate. In the final results, this is not necessary since B_t^G never drops below 0.5. But having a well-defined tax rate in negative B_t^G regions helps in the early computation stages. So, $\underline{B}^G$ is a purely technical parameter. Given its value, we then set b^G to target the volatility of government debt to GDP. In the data (53-14), it is 10.96%. In the model, it is 12.39%.

REFERENCES

ANDREWS, I., M. GENTZKOW, AND J. M. SHAPIRO (2017): "Measuring the Sensitivity of Parameter Estimates to Estimation Moments," *Quarterly Journal of Economics*, 132, 1553–1592. [17]

BARON, M. (2020): "Countercyclical Bank Equity Issuance," *Review of Fiancial Studies*, 33, 4186–4230. [13]

BRUMM, J., D. KRYCZKA, AND F. KUBLER (2018): "Recursive Equilibria in Dynamic Economies With Stochastic Production," *Econometrica*, 85, 1467–1499. [1]

ELENEV, V. (2016): "Mortgage Credit, Aggregate Demand, and Unconventional Monetary Policy," Working Paper. [9]

GUERRIERI, L., AND M. IACOVIELLO (2015): "Occbin: A Toolkit to Solve Models With Occasionally Binding Constraints Easily," *Journal of Monetary Economics*, 70, 22–38. [1]

JUDD, K. L. (1998): *Numerical Methods in Economics*. The MIT Press. [1]

JUDD, K. L., F. KUBLER, AND K. SCHMEDDERS (2002): "A Solution Method for Incomplete Asset Markets With Heterogeneous Agents," Working Paper, SSRN. [8]

KRISHNAMURTHY, A., AND A. VISSING-JORGENSEN (2015): "The Impact of Financial Supply on Financial Sector Lending and Stability," *Journal of Financial Economics*, 118, 571–600. [14]

KUBLER, F., AND K. SCHMEDDERS (2003): "Stationary Equilibria in Asset-Pricing Models With Incomplete Markets and Collateral," *Econometrica*, 71, 1767–1793. [9]

ROUWENHORST, G. (1995): "Asset Pricing Implications of Equilibrium Business Cycle Models," in *Frontiers of Business Cycle Research*, ed. by Cooley. Princeton University Press. [2,9]

Co-editor Giovanni L. Violante handled this manuscript.

Manuscript received 20 June, 2018; final version accepted 9 October, 2020; available online 22 October, 2020.